

FI-ODE: Certified and Robust Forward Invariance in Neural ODEs

Yujia Huang *
Caltech

Ivan Dario Jimenez Rodriguez *
Caltech

Huan Zhang
CMU

Yuanyuan Shi
UCSD

Yisong Yue
Caltech

Abstract

We study how to certifiably enforce forward invariance properties in neural ODEs. Forward invariance implies that the hidden states of the ODE will stay in a “good” region, and a robust version would hold even under adversarial perturbations to the input. Such properties can be used to certify desirable behaviors such as adversarial robustness (the hidden states stay in the region that generates accurate classification even under input perturbations) and safety in continuous control (the system never leaves some safe set). We develop a general approach using tools from non-linear control theory and sampling-based verification. Our approach empirically produces the strongest adversarial robustness guarantees compared to prior work on certifiably robust ODE-based models (including implicit-depth models).

1 Introduction

Deployment of neural networks in the real-world increasingly demands formal certificates of performance, often under malicious inputs. Examples of certified behaviors include correctly classifying samples despite perturbations on their inputs, and controlling a dynamical system to stay inside a safe set. Provably certifying the behavior of a network is important given that even impressive empirical robustness techniques can often be defeated by stronger attacks [5], and we desire assurances that can be useful in applications with strong reliability requirements.

We are interested in leveraging control-theoretic concepts, such as Lyapunov stability and forward invariance, to design neural networks with such certified behaviors. These concepts have been successfully used to certify dynamical systems, both in terms of safety [3] as well as robustness under adversarial perturbations [27]. We focus on the neural ODE function class [21, 16, 9], which is a natural starting point for incorporating control-theoretic tools (cf. [45, 25, 28, 23]). Here, forward invariance guarantees that the states of the neural ODE never leaves some “good” region,

which under suitable instantiations can produce robustness guarantees for classification or safety guarantees for control.

Our contributions: We present FI-ODE, a general approach for training certifiably forward invariant neural ODEs. Our framework can use “good” regions that are defined both explicitly and implicitly (via data), and can be applied to high-dimensional inputs (images) as well as dynamic control systems. Our technical contributions are:

- We develop a robustness guarantee based on a forward invariance condition of sub-level sets of Lyapunov functions. One can train a neural ODE such that a task-specific cost function (e.g., cross-entropy loss in image classification, or state-based cost in continuous control) becomes the associated Lyapunov function for the ODE, allowing us to invoke the robustness guarantee. In this case, the “good” region to be (robustly) forward invariant to is implicitly defined in a data-driven way.
- We constrain the hidden states of a neural ODE using a Control-Barrier Function based Quadratic Program [3] implemented as an optimization layer [1]. We can use this layer to explicitly constrain the states to lie in a compact set, which is useful for certification.
- We develop an adaptive robust Lyapunov training algorithm tailored to efficient certification. Compared to standard Lyapunov training [23], the algorithm focuses on the boundary of the “good” region, which is crucial to certifying robust forward invariance.
- We develop a verification method through a combination of efficient sampling and a new interval propagation technique compatible with optimization layers, which can be incorporated into existing neural network verification methods such as CROWN [47].

We empirically show superior ℓ_2 certified robustness compared to all other certifiably robust ODE-based models (including implicit depth models such as Deep-Equilibrium models [10]) on MNIST and CIFAR-10. We also demonstrate the generality of our approach by applying it to nonlinear control problems, where we train and certify neural ODE policies to keep the system within a safe region. Our code is available at <https://github.com/yjhuangcd/FI-ODE.git>.

* Authors contributed equally.

2 Preliminaries

In this section we introduce neural ODEs and control-theoretic properties of ODEs such as stability and forward invariance. We provide sufficient conditions for ODEs to achieve these properties along with methods for training Neural ODEs satisfy these conditions. Finally, we place these properties in the adversarial robustness setting.

Neural ODE Model Class. The forward pass of a neural ODE parameterized by $\theta \in \Theta \subseteq \mathbb{R}^l$ is defined as follows:

$$\eta(0) = \phi_\theta(x), \quad (\text{input layer}) \quad (1a)$$

$$\frac{d\eta}{dt} = f_\theta(\eta(t), x), \quad (\text{continuum of hidden layers}) \quad (1b)$$

$$\hat{y} = \psi_\theta(\eta(t)). \quad (\text{output layer}) \quad (1c)$$

Equations (1a) to (1c) approximate a mapping from an input x to a label y , where $x \in \mathbb{R}^n$, $\eta \in \mathcal{H} \subset \mathbb{R}^k$ and $y \in \mathbb{R}^m$. The state space for the hidden layer ODE \mathcal{H} , is assumed to be compact and connected. The system evolves over $t \in [0, T]$ and, although $\hat{y}(t)$ can be evaluated on any t in this range, the final prediction is $\hat{y}(T)$.

2.1 Stability, Forward Invariance, and Learnability

Lyapunov Stability. In general, dynamical systems can be chaotic: small changes in initial conditions can result in large changes to the resulting trajectories. In contrast, stable systems are well behaved in that small changes to initial conditions result in small changes to the trajectories. This is a particularly desirable property in the context of robustness since these small changes to initial conditions can be interpreted as adversarial perturbations. Formally, we define stability using a continuously differentiable potential function $V : \mathbb{R}^k \rightarrow \mathbb{R}_{\geq 0}$ and class \mathcal{K} function $\bar{\sigma} : \mathbb{R}_{\geq 0} \rightarrow [0, \infty)$ so that $V(\eta) \leq \bar{\sigma}(\|\eta\|)$ for some norm $\|\cdot\|$.⁰ In the classification case, the potential function V can be the cross entropy function if the ODE's outputs \hat{y} are the logits.

Definition 1 (Stability). A flow field of the form shown in eq. (1b) is stable with respect to a potential function V if for all initial conditions $\eta(0) \in \mathcal{R} \subset \mathcal{H}$ the flow satisfies $V(\eta(t)) \leq e^{-\kappa(t)} V(\eta(0))$ where $\kappa : \mathbb{R}_{\geq 0} \rightarrow [0, \infty)$ is a class \mathcal{K} function. We refer to \mathcal{R} as the region of attraction.

When a potential function V satisfies Definition 1, we call V a Lyapunov function for that ODE. A common choice is $V^{sq}(\eta) = \|\eta - \eta^*\|_2^2$ and shape the ODE such that V^{sq} is a Lyapunov function (either because the ODE is overparameterized or controllable). In this case, the equilibrium point is η^* , and the distance between the current state η and η^* decreases exponentially fast. Once reaching η^* , the system stays at η^* forever. Note that in general, one can stabilize to

⁰Specifically, a scalar $\bar{\sigma}$ is class \mathcal{K} if it is strictly increasing, continuous, and has $\bar{\sigma}(0) = 0$. See appendix for a full definition.

a subset of the state space rather than a single equilibrium point.

Control Lyapunov Functions. Control Lyapunov Functions (CLFs) provide necessary and sufficient algebraic conditions to enforce stability in a given dynamical system [4]. In particular, we have a local state-based inequality that, if true everywhere in the region of attraction \mathcal{R} , implies stability. Intuitively, if the time derivative of the potential function V is sufficiently negative, the system is stable:

Theorem 2.1 (Exponentially Stabilizing Control Lyapunov Function (ES-CLF) Implies Exponential Stability ([4])). *For the ODE in eqs. (1a) to (1c), a continuously differentiable function $V : \mathbb{R}^k \rightarrow \mathbb{R}_{\geq 0}$ is an ES-CLF if there are class \mathcal{K} functions $\bar{\sigma}$ and κ such that:*

$$V(\eta) \leq \bar{\sigma}(\|\eta\|), \quad (2)$$

$$\min_{\theta \in \Theta} \left[\frac{\partial V}{\partial \eta} \bigg|_{\eta} f_\theta(\eta, x) + \kappa(V(\eta)) \right] \leq 0 \quad (3)$$

holds for all $\eta \in \mathcal{R} \subseteq \mathcal{H}$ and $t \in [0, 1]$. The existence of an ES-CLF implies that there is a $\theta \in \Theta$ that can achieve:

$$\frac{\partial V}{\partial \eta} \bigg|_{\eta} f_\theta(\eta, x) + \kappa(V(\eta)) \leq 0, \quad (4)$$

and furthermore the ODE using θ is exponentially stable with respect to V , i.e., $V(\eta(t)) \leq V(\eta(0))e^{-\kappa t}$.

Forward Invariance. We can generalize the concept of equilibrium points to sets using forward invariance: once the system enters the desired set it remains inside for all time. In the classification setting, interesting sets include states that correspond to valid probability distributions or states that produce a correct classification.

Definition 2 (Forward Invariance). A set $\mathcal{S} \subseteq \mathcal{H}$ is forward invariant if $\eta(t) \in \mathcal{S} \Rightarrow \eta(t') \in \mathcal{S}, \forall t' \geq t$.

Lyapunov Sublevel Sets. Lyapunov sublevel sets provide one way to define forward invariant sets. Given a Lyapunov Function V and a positive constant c , a Lyapunov sublevel corresponds to all states where V is c or less (i.e. $\{\eta \in \mathcal{H} | V(\eta) \leq c\}$). Since a Lyapunov function V is always decreasing in time, once a state enters a Lyapunov sublevel set it remains there for all time.

Control Barrier Functions. In a similar fashion to CLFs, Control Barrier Functions (CBFs) provide algebraic conditions to verify that an ODE renders a set forward invariant.

Theorem 2.2 (Control Barrier Function (CBF) Implies Forward Invariance [44, 30]). *Let the set $\mathcal{S} \subset \mathcal{H}$ be the 0 superlevel set of a continuously differentiable function $h : \mathcal{H} \rightarrow \mathbb{R}$, i.e. $\mathcal{S} = \{\eta \in \mathcal{H} | h(\eta) \geq 0\}$. The set \mathcal{S} is forward invariant with respect to the ODE eqs. (1a) and (1b), if h satisfies either of the following conditions:*

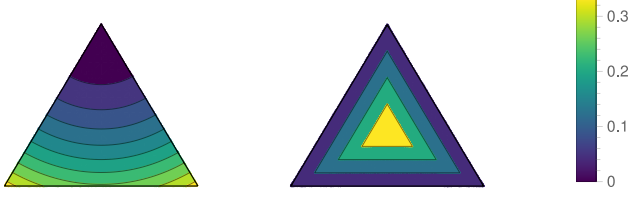


Figure 1: Depicting a comparison of Lyapunov and barrier functions in the simplex for 3 classes. The triangle shows the simplex projected to a plane. The color contours show level-sets of a potential function V (left) and of a barrier function h (right). The function V would stabilize the system towards the top class. On the right we show a barrier function for the simplex: $h(\eta) = \min_i \eta_i$. A dynamical system that evolves in the simplex renders the the simplex ($\{\eta \in \mathcal{H} | h(\eta) \geq 0\}$) forward invariant (i.e., stays in the simplex for all time).

1. ([44]) There exists a function α for all $\eta \in \mathcal{H}$ so that:

$$\max_{\theta \in \Theta} \left[\frac{\partial h}{\partial \eta} \bigg|_{\eta} f_{\theta}(\eta, x) + \alpha(h(\eta)) \right] \geq 0, \quad (5)$$

where α is a class \mathcal{K}_{∞}^e function (this means $\alpha : \mathbb{R} \rightarrow \mathbb{R}$ is strictly increasing and satisfies $\lim_{r \rightarrow \infty} \alpha(r) = \infty$).

2. ([30]) For all $\eta \in \{\eta \in \mathcal{H} | h(\eta) = 0\}$:

$$h(\eta) = 0 \text{ implies } \frac{\partial h}{\partial \eta} \neq 0. \quad (6a)$$

$$\max_{\theta \in \Theta} \left[\frac{\partial h}{\partial \eta} \bigg|_{\eta} f_{\theta}(\eta, x) \right] \geq 0. \quad (6b)$$

Comparing Forward Invariance Constructions. Figure 1 highlights the difference defining Forward Invariance using Lyapunov vs. Barrier functions. Lyapunov stability implies the system stabilizes towards a point (in this case the top corner), so a system inside Lyapunov sublevel continues to stabilize, hence is forward invariant. When using Barrier functions, a set of “good” or *safe* states is defined as the 0-super level set a potential function h : $\{\eta \in \mathcal{H} | h(\eta) \geq 0\}$.¹

ES-CLF and CBF as learnability conditions. Both the ES-CLF and CBF conditions can be viewed as learnability properties of neural ODEs [23]. The ability to satisfy eqs. (3), (5) and (6) implies the existence of a $\theta \in \Theta$ that results in stability or forward invariance. Therefore, certifying stability or forward invariance reduces to finding θ that satisfy eqs. (3), (5) and (6) over the state space.

2.2 Lyapunov Training of Neural ODEs

One way to train Neural ODEs to satisfy control-theoretic conditions in eqs. (3), (5) and (6) is to define a loss that

¹Here we must disambiguate the functions h and V from a CBF and ES-CLF. In both cases, the function formally specifies the desirable property such as what point we wish to be stable to while CBFs and ES-CLFs specify an algebraic condition the function satisfies in conjunction with the dynamics to actually achieve the property.

penalizes violations, as presented in the Lyapunov Loss [23], which uses a hinge-like loss on violations of eq. (3).

Definition 3 (Lyapunov Loss [23]). For the ODE defined in eqs. (1a) to (1c) and a dataset of input-output pairs $(x, y) \sim D$ the Lyapunov Loss is defined as:

$$\mathcal{L}(\theta) := \mathbb{E}_{(x, y) \sim D} \left[\int_0^T \max \left\{ 0, \frac{\partial V}{\partial \eta} \bigg|_{\eta} f_{\theta}(\eta, x) + \kappa V(\eta) \right\} dt \right]. \quad (7)$$

A corresponding Barrier Loss [33] can be defined analogously (see supplementary materials). Clearly, if eq. (7) is zero, then the condition in eq. (3) is satisfied. Although a zero loss implies exponential convergence (i.e. a low final classification loss), the integral makes computing eq. (7) difficult. Instead we can approximate the internal integral by sampling over the system’s state space. This leads to the Monte Carlo Lyapunov loss [23]:

$$\mathcal{L}(\theta) \approx \mathbb{E}_{\substack{(x, y) \sim D \\ \eta \sim \mu(\mathcal{H})}} \left[\max \left\{ 0, \frac{\partial V}{\partial \eta} \bigg|_{\eta} f_{\theta}(\eta, x) + \kappa V(\eta) \right\} \right]. \quad (8)$$

The remaining design choice is the distribution μ , which was simply the uniform distribution in [23] and may require an intractable number of samples to minimize eq. (8) everywhere. In Section 3.3, we introduce an adaptive sampling approach that can lead to much more efficient training.

2.3 Adversarial Robustness

The previous definitions assume no perturbations on the system’s input. Suppose instead that a possibly adversarially chosen corruption $\epsilon \in \mathbb{R}^n$ with $\|\epsilon\|_2 \leq \bar{\epsilon}$ gets added to the input part of the input-output pair (x, y) . Assuming that x produces a correct prediction, we aim to provably guarantee through forward invariance that all predictions based on $x + \epsilon$ will also produce the same or similar predictions. This property is known as certified adversarial robustness [42, 32, 38, 11, 6], and is particularly challenging to achieve when dealing with high-dimensional inputs such as images.

3 Forward Invariance for Neural ODE

We now present our FI-ODE framework to enforce forward invariance on neural ODEs (see Figure 2). We consider two ways mirroring the two constructions in Section 2.1: project the dynamics to satisfy the CBF conditions; and train the dynamics with a loss that penalizes the violation of the forward invariance conditions (using the Lyapunov Loss construction in Equation (7)) and then verify that the conditions hold on the level set of the potential function. In Section 3.1, we concatenate a projection layer after the neural network so that the dynamics keep the states on a

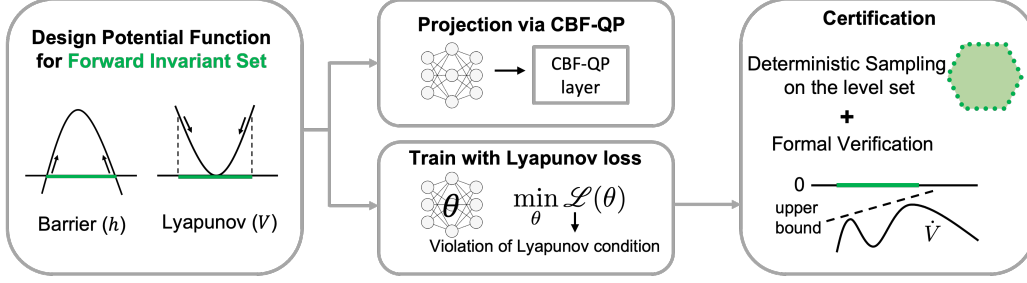


Figure 2: Overview of our FI-ODE framework. We first design the potential function based on the shape of the forward invariant set. Then we enforce the forward invariance property on neural ODE by projecting the dynamics to satisfy CBF condition or training the dynamics with Lyapunov loss and certifying afterwards.

probability simplex, which is a natural choice of the state space for the image classification problem. In Section 3.2, we formulate robust forward invariant conditions via Lyapunov level sets. In Section 3.3 and Section 3.4, we develop effective training and certification algorithms, respectively.

3.1 Forward Invariance on a Simplex via Projection

For the purposes of certification and training, it is often useful to make \mathcal{H} be a bounded set, as certifying over unbounded sets is typically intractable. For image classification, a natural choice of the bounded set is the probability simplex, i.e., η evolves in the simplex and the output layer ψ is the identity function. Recall that the simplex is defined as $\Delta = \{\eta \in \mathbb{R}^n \mid \sum_{i=1}^n \eta_i = 1, \eta_i \geq 0\}$. We can choose the initial condition to be the constant function $\phi(x) = \mathbb{1} \frac{1}{n}$ so that the η starts in the simplex.

Since the initial condition is defined to be in the simplex, it suffices to derive a set of barrier conditions render the simplex forward invariant. We define a set of n barrier functions, $h_i(\eta) = \eta_i$ such that $\{\eta \mid \eta_i \geq 0\}$ is the 0-superlevel set of h_i . It follows from Theorem 2.2 that each of these barrier functions must satisfy $\frac{dh_i}{d\eta} f(\eta, x, t) \geq -\alpha(h_i(\eta))$ for some class \mathcal{K}_∞ function α . This constraint set can be alternatively expressed as $f(\eta, x, t) \geq -\alpha(\eta)$.

Then we consider the summation constraint for the simplex, $\sum_{i=1}^n \eta_i = 1$. By taking a time derivative of both sides, we have the constraint on the dynamics: $\frac{d}{dt} (\sum_{i=1}^n \eta_i(t)) = \sum_{i=1}^n f_{\theta}(\eta, x, t)_i = \mathbb{1}^\top f_{\theta}(\eta, x, t) = 0$.

We explicitly constrain η to evolve on simplex using an optimization layer [1]. Specifically, we pass an unbounded neural network $\hat{f}(\eta, x, t)$ through a Control Barrier Function Quadratic Program (CBF-QP) Safety Filter [20]:

$$\begin{aligned} f(\hat{f}) &= \underset{\mathbf{f} \in \mathbb{R}^k}{\operatorname{argmin}} \frac{1}{2} \|\mathbf{f} - \hat{f}\|_2^2, \\ \text{s.t.} \quad &\mathbb{1}^\top \mathbf{f} = 0, \\ &\mathbf{f} \geq -\alpha(\eta), \end{aligned} \quad (9)$$

where the arguments to the function \hat{f} are omitted for brevity.

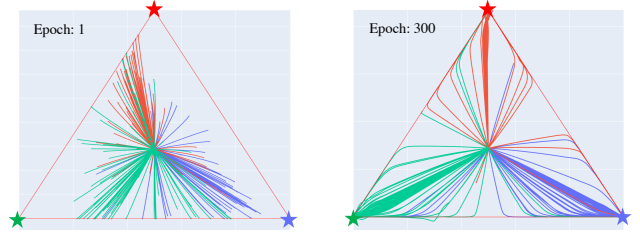


Figure 3: Depicting ODE trajectories that satisfy the simplex constraint for CIFAR-3 on epochs 1 and 300. Each colored line represents the trajectory of an input example of a specific class, and the stars at the corners are colored with the ground-truth class.

To learn in this setting we differentiate through the QP using the KKT conditions as shown in [1]. Given the simple nature of the QP, we implemented a custom solver that uses binary search to efficiently compute solutions, detailed in supplementary materials.

To demonstrate the effectiveness of the CBF-QP layer, we visualize the learned trajectories on the CIFAR-3 dataset (a subset of CIFAR-10 with the first 3 classes) in Figure 3. As training progresses, the trajectories are trained to evolve to the correct classes. All the trajectories stay in the simplex, validating that the learned dynamics satisfy the constraints in CBF-QP Equation (9).

3.2 Certified Robustness via ES-CLF

Our method for certifying the adversarial robustness of a data sample x relies on verifying that a Lyapunov stability condition holds over bands of level sets of the potential

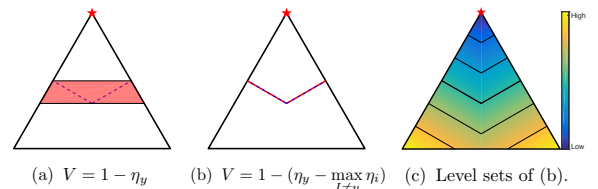


Figure 4: Lyapunov functions and their level sets on a 3-class probability simplex. The red star is the correct class.

function V_y as shown in Figure 4. As discussed in Section 2.1, this Lyapunov condition not only certifies forward invariance of the regions of the state space that guarantee correct classification, but provably ensures the dynamics will evolve from the initial condition to the region of correct classification in finite time. For the special case where the Lyapunov function corresponds to the margin, we certify that condition Equation (6) holds everywhere on the level set corresponding to the decision boundary.

Theorem 3.1 (ES-CLF in Band Implies Robust Correct Classification). *Consider the dynamical system in Equations (1a) to (1c) with dynamics restricted to the simplex as shown in Equation (9) and initial condition satisfying $\eta(0) \in \Omega_{\bar{V} \setminus \underline{V}} = \{\eta \in \Delta | \underline{V} \leq V(\eta) \leq \bar{V}\}$ where V satisfies the conditions on Theorem 2.1 and condition Equation (3) holds for all $\eta \in \Omega_{\bar{V} \setminus \underline{V}}$. If the following conditions hold then $\eta(T)$ will produce a correct classification of input-output pair $(x + \epsilon, y)$:*

1. **Sufficient Exponential Stability:** The exponential convergence constant κ satisfies

$$\kappa \geq \frac{\bar{\epsilon} L_V L_f^x}{\underline{V}} \quad (10)$$

where $\bar{\epsilon}$ is the perturbation magnitude on the input, L_V is the Lipschitz constant of the Lyapunov function, and L_f^x is the Lipschitz constant of the dynamics with respect to x .

2. **Sufficient Integration Time:**

$$T \geq -\frac{1}{\kappa} \ln \left(\frac{\underline{V} - \frac{L_V L_f^x}{\kappa}}{V(\eta(0)) - \frac{L_V L_f^x}{\kappa}} \right) \quad (11)$$

3. **Lower Bound Correctly Classifies:** $V(\eta) \leq \underline{V}$ implies η correctly produces a correct classification.

See supplementary material for proof.

In practice, we can choose different CLFs which lead to different conditions for certified robustness. We give two examples: a) maximum likelihood Lyapunov function and b) margin Lyapunov function (Figure 1).

Maximum likelihood (MLL) Lyapunov function. We define the MLL Lyapunov function to be $V_y = 1 - \eta_y$, where y is the correct label. This Lyapunov function only depends on the state corresponding to the correct label. For a 3-class classification problem with initial condition $[\frac{1}{3}, \frac{1}{3}, \frac{1}{3}]$, we choose $\bar{V} = 1 - \frac{1}{3} = \frac{2}{3}$ and $\underline{V} = 1 - \frac{1}{2} = \frac{1}{2}$ such that the decision boundary $\mathcal{D} = \{\eta | \eta_y = \max_{i \neq y} \eta_i, \eta \in \Delta\}$ lies in $\Omega_{\bar{V} \setminus \underline{V}} = \{\eta \in \Delta | \frac{1}{3} \leq \eta_y \leq \frac{1}{2}\}$. The region of $\Omega_{\bar{V} \setminus \underline{V}}$ is denoted by red in Figure 4. If the conditions in Theorem 3.1 hold for all $\eta \in \Omega_{\bar{V} \setminus \underline{V}}$, then for all perturbed inputs starting from the initial states, the trajectories pass through the

red region and stay forward invariant in the region where $\eta_y \geq \frac{1}{2}$, therefore guarantees correct classification.

Margin Lyapunov function. The above Lyapunov function leads to conditions that are more strict than correct classification because $\{\eta \in \Delta | V_y(\eta) \leq \underline{V}\}$ is a strict subset of the decision region of class y . In contrast, the margin Lyapunov function has level sets that are parallel to the decision boundary. We define the margin Lyapunov function as $V_y = 1 - (\eta_y - \max_{i \neq y} \eta_i)$. The 1-level set of V_y , $\{\eta \in \Delta | V_y(\eta) = 1\}$ is the decision boundary $\mathcal{D}_y = \{\eta \in \Delta | \eta_y = \max_{i \neq y} \eta_i\}$. Therefore, we pick $\bar{V} = \underline{V} = 1$. If the conditions in Theorem 3.1 holds, the trajectories stays in the correct decision region.

3.3 Adaptive Robust Lyapunov training

Our learning algorithms build upon the Lyapunov training framework in [23] and are summarized in Algorithm 1.

Adaptive sampling. Our learning strategy is to minimize the Lyapunov Loss (Equation (8)), which guarantees that the Lyapunov condition holds everywhere the system evolves. The Monte Carlo Lyapunov Loss approximates this integral with a finite number of samples. This leads to a challenge of how to train efficiently with the Lyapunov Loss since Monte Carlo scales poorly with the dimensionality of the integral.

We address this challenge with an adaptive sampling strategy that focuses the training samples on regions of the state space that are crucial for satisfying forward invariance: the boundary of the Lyapunov sub-level set. We adapt the sampling distribution as training progresses. We start by sample uniformly in a hypercube or hypersphere towards the origin as in [23] since trajectories an untrained neural ODE can visit anywhere in the state space (see example in Figure 3). As training progresses, we concentrate sampling on the forward invariant set (the sublevel set of the CLF and the superlevel set of the CBF). This process focuses the sampling on regions most important for certifying robust forward invariance.

Restricting Lipschitz constant. Another challenge to obtain non-vacuous robustness bound is to ensure κ to be larger than a threshold which depends on L_f^x (see sufficient exponential stability condition in Equation (10)). In practice, the Lipschitz bound of a small neural network for image classification can be on the order of 10^8 , and it is unfeasible to train with such a large κ in the Lyapunov Loss. Therefore, we need to restrict the Lipschitz constants of the learned dynamics with respect to the input x . In addition, since we rely on the smoothness of the dynamics to verify the Lyapunov condition holds on the region of interest (Section 3.4), we also need to restrict the Lipschitz constant with respect to η to ensure the dynamics do not change excessively for two states that are close.

To control the Lipschitz constant of our neural network dy-

Algorithm 1: Adaptive Robust Lyapunov training.

Input : Lyapunov function V , Sampling scheduler, dataset \mathcal{D} , perturbation magnitude $\bar{\epsilon}$.

Initialize : Model parameters θ .

for $i=1:M$ **do**

$(x, y) \sim \mathcal{D}$
 \triangleright Sample η based on the training progress and the level sets.
 $\eta \sim \text{Sampling_scheduler}(i, V)$
 \triangleright Set κ based on the Lipschitz and $\bar{\epsilon}$ (Equation (10))
 $\kappa = \frac{\bar{\epsilon} L_V L_f^x(\theta)}{V}$
 \triangleright Update model parameters to minimize Lyapunov loss.
 $\psi = \max \left\{ 0, \frac{\partial V}{\partial \eta} \Big|_{\eta} f_{\theta}(\eta, x) + \kappa V(\eta) \right\}$
 $\theta \leftarrow \theta - \beta \nabla_{\theta} \sum_j \psi(\theta, \eta_j, x, y)$

return θ

namics, we use orthogonal layers [37] and training with a Lipschitz bound in the loss [38]. We find that both methods perform similarly, but using orthogonal layers is more computationally efficient and less sensitive to hyper-parameters.

3.4 Certification

Procedure and challenges The certification procedure is as follows: 1) sampling points on the boundary of the level set, 2) check Lyapunov condition holds on all the sampled points, and 3) perturb around each sampled point and verify the condition holds in a small neighborhood around those points. There are two key challenges to address in order to make this approach rigorous and practical. First, we need to construct a set of samples that cover the whole level set boundary. Second, our neural ODE architecture consists of standard neural network layers and a CBF-QP layer. However, existing verification tools (for a single point) that rely on interval propagation (an over-estimate of the range of values the layers can take) do not apply to optimization layers such as a CBF-QP. We address both challenges.

Sampling in a simplex and on the decision boundary.

For image classification tasks, the boundary of the Lyapunov level set is the decision boundary on a simplex. Naive sampling in a hypercube rarely gives us samples that are on the simplex. Therefore, we develop tools for deterministic sampling on the simplex and on the decision boundary. In Theorem 3.2, we first give the construction of the sample set. Then we show that the constructed set can cover the whole simplex or decision boundary by showing that, given any point on the simplex or decision boundary (red dot in Figure 5), there exists a sampled point close by (blue dot).

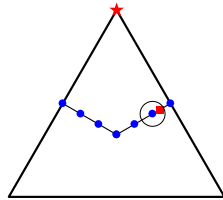


Figure 5: Sampling to cover the whole decision boundary.

Theorem 3.2. (a) Sampling in a simplex. For $T \in \mathbb{Z}_+$, let $S = \{s \in \mathbb{Z}^n \mid \sum_{i=1}^n s_i = T, s_i \geq 0, \forall i = 1, \dots, n\}$ and $\tilde{S} = \{\tilde{s} \in \mathbb{R}^n \mid \tilde{s} = \frac{s}{T}, s \in S\}$. For any $\eta \in \Delta$, there exists an $\tilde{s} \in \tilde{S}$ such that $|\eta_i - \tilde{s}_i| \leq \frac{1}{T}$ for all $i = 1, \dots, n$.

(b) Sampling on the decision boundary. For $T \in \mathbb{Z}_+$, $T \equiv 0 \pmod{2}$ and $T \not\equiv 1 \pmod{n}$, let $S_y = \{s \in \mathbb{Z}^n \mid \sum_{i=1}^n s_i = T, s_y = \max_{i \neq y} s_i, s_i \geq 0, \forall i = 1, \dots, n\}$, and $\tilde{S}_y = \{\tilde{s} \in \mathbb{R}^n \mid \tilde{s} = \frac{s}{T}, s \in S_y\}$. For any $\eta \in \mathcal{D}_y$, there exists an $\tilde{s} \in \tilde{S}_y$ such that $|\eta_i - \tilde{s}_i| \leq \frac{1}{T}$ for all $i = 1, \dots, n$.

Remark. The cardinality of the set S is $\binom{T+n-1}{n-1}$. In contrast, sampling in a hyper-cube $[0, 1]^n$ with T points each dimension leads to T^n samples.

In practice, we construct the decision boundary set \tilde{S}_y via dynamic programming. See supplementary for the details.

Rejection sampling. For general potential functions, it is not straightforward on how to do uniform deterministic sampling on the level set. For instance, the common Lyapunov function $V^{sq}(\eta) = \|\eta - \eta^*\|_2^2$ has sphere level sets, and it is non-trivial to generate uniform deterministic samples on a sphere [46]. In this case, we sample in the ambient space first, and then find two level sets that surrounds the targeted level set and reject the points outside the two level sets.

Interval bound propagation through CBF-QP layer.

The dynamics of our neural ODE is parameterized by a neural network followed by a CBF-QP layer. Let \hat{f} be the dynamics after the neural network, and let $f(\hat{f})$ be the dynamics after CBF-QP layer. To bound $f(\hat{f})$, we first bound \hat{f} using a popular linear relaxation based verifier named CROWN [47]. However, CROWN does not support perturbation analysis on differentiable optimization layers such as our CBF-QP layer and deriving linear relaxation for CBF-QP can be hard. However, it is possible to derive interval bounds (a special case of linear bounds in CROWN) through CBF-QP. Consider a QP in the form of (9):

$$\begin{aligned}
 f(\hat{f}) &= \underset{\mathbf{f} \in \mathbb{R}^n}{\operatorname{argmin}} \frac{1}{2} \|\mathbf{f} - \hat{f}\|_2^2 \\
 \text{s.t.} \quad & \mathbb{1}^\top \mathbf{f} = b \\
 & \underline{f}(\eta) \leq \mathbf{f} \leq \bar{f}(\eta)
 \end{aligned} \tag{12}$$

where \underline{f} and \bar{f} are non-increasing function of η . We can bound each dimension of $f(\hat{f})$ in $\mathcal{O}(n)$ by setting the corresponding element of the input to the lower or upper bound. Mathematically, define function h_i to be $h_i : \eta, \hat{f} \mapsto f(\hat{f})_i$. Given perturbed input in an interval bound $\underline{\hat{f}}_i \leq \hat{f}_i \leq \bar{\hat{f}}_i$, we have

$$h_i(\eta_{ub}^i, \bar{\hat{f}}_{lb}^i) \leq f(\hat{f})_i \leq h_i(\eta_{lb}^i, \underline{\hat{f}}_{ub}^i) \tag{13}$$

where η_{ub}^i, η_{lb}^i are defined as follows and f_{ub}^i, f_{lb}^i are defined similarly:

$$\eta_{ub}^i = \begin{cases} \overline{\eta_j}, & j = i \\ \underline{\eta_j}, & j \neq i \end{cases} \quad \eta_{lb}^i = \begin{cases} \eta_j, & j = i \\ \overline{\eta_j}, & j \neq i \end{cases} \quad (14)$$

4 Experiments

We evaluate our FI-ODE approach on two applications: 1) certified robustness for image classification (section 4.1), and 2) safety in continuous control (section 4.2). In the ablation studies, we compare different learning and certification algorithms (section 4.3).

4.1 Certified Robustness for Image Classification

We evaluate on standard benchmarks, by perturbing the input images within an ℓ_2 ball of radius 0.1 and 0.2 on MNIST, and 36/255 on CIFAR-10. Our goal is to evaluate the effectiveness of our FI-ODE approach for training certifiably robust Neural ODEs. To our knowledge, there are no previous works demonstrating certified robustness of Neural ODEs on CIFAR-10. Therefore, we compare with methods on certifying robustness of monotone deep equilibrium models (monDeq) [31, 10]. Similar to Neural ODE, MonDeq [41] is also an implicit-depth model.

Table 1 shows the results. The main metric is certified accuracy, the percentage of test set inputs that are certifiably robust. Our method significantly outperforms Lipschitz-MonDeq [31] on both MNIST and CIFAR-10. High variance makes direct comparison with Semialgebraic-MonDeq [10] results difficult since they only include 100 test images on MNIST due to their high computational cost. Our method performs similarly if not better when comparing accuracy within 95 % confidence interval. These results suggest that our FI-ODE approach achieves the strongest overall certified robustness results compared to prior ODE-based approaches.

4.2 Certifying Safety for Continuous Control

We test our approach on a planar segway system with three states: angular position ϕ , angular velocity $\dot{\phi}$ and velocity v . Our goal is to train a neural ODE controller and certify that the controller keeps the states in a forward invariant safe set.

We enforce forward invariance within the c -sublevel set of the Lyapunov function: $\Omega_c(V) = \{x | V(x) \leq c\}$. We learn a quadratic Lyapunov function $V(x) = x^T P x$, where P is positive definite and learnable, and use adversarial training to increase the penalty for states that tend to violate the Lyapunov condition. Adversarial training is useful to restrict the empirical Lipschitz of the dynamics and eases the certification. During certification, we use rejection sampling to find

Table 1: ℓ_2 certified robustness. Accuracy (%) is reported. Semi-MonDeq results are reported on 100 test images with 95 % confidence interval due to high cost, and 10,000 test images are used for other methods.

Dataset	Method	ϵ	Clean	Certified
MNIST	Lipschitz-MonDeq [31]		95.6	83.09
	Semi-MonDeq [†] [10]	0.1	99 [>94]	99 [>94]
	Robust FI-ODE (Ours)		99.35	95.75
CIFAR-10	Lipschitz-MonDeq [31]	0.2	95.6	50.56
	Robust FI-ODE (Ours)		99.35	81.65
	Robust FI-ODE (Ours)	0.141	78.34	42.27

Table 2: Ablation study for robust FI-ODE training.

Training Method	Clean	AutoAttack	Certified
w/o Lyapunov training	69.05	56.94	16.81
w/o Sampling scheduler	73.15	64.87	41.43
w/o Lipschitz restriction	82.83	74.81	0
Robust FI-ODE (ours)	78.34	67.45	42.27

the states that cover the c -level set of the Lyapunov function (states between the two dashed lines in fig. 6), check that $\dot{V} < 0$ holds on those states, and use CROWN [32] to verify the condition also holds around a neighborhood of the sampled states. Then we can show that the set within the solid line is forward invariant.

Figure 6 (a) shows the contours of the time derivative of the learned Lyapunov function on two of the three dimensions when $v = 0$. The solid line is the level set when $V = 0.15$. The two dashed lines show the region where samples are accepted during rejection sampling. Figure 6 (b) shows trajectories with initial states in the forward invariant set (the gray ellipsoid).

4.3 Ablation Studies

For all ablation studies we consider robust image classification on the CIFAR-10 dataset. Table 2 compares the effects that different components of the FI-ODE training procedure have on the clean, empirical adversarial (evaluated using AutoAttack [12]) and certified accuracy of the model. We see that all the learning components: Lyapunov training, adaptive sampling and Lipschitz restriction are indispensable to good performance. Without Lipschitz restriction, the global Lipschitz bound of the dynamics is on the order of 10^8 , making the robustness guarantee vacuous. The high empirical adversarial accuracy is mostly due to gradient obfuscation, since the adversarial accuracy drops the most after a non-gradient based attack (square attack).

Table 3: Computational costs of certification methods.

Certification Method	Lyapunov function	Sampling Method	# samples	Time (s)	Certified
Lipschitz	Margin	Decision Boundary	4.13×10^7	2.8	33.46
CROWN	MLL	Simplex	5.66×10^8	6180	5.92
CROWN	Margin	Decision Boundary	4.13×10^7	240	42.27

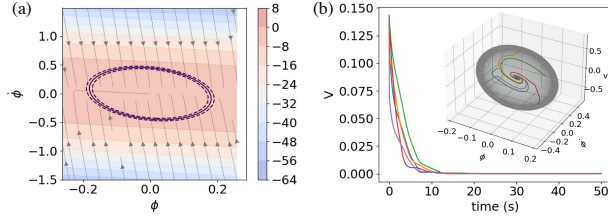


Figure 6: (a) \dot{V} contours and certified forward invariant set (within the solid line). Background gray arrows are the dynamic flows. (b) V along the trajectories. All trajectories starting within the forward invariant set stay in it.

Table 3 compares the computational costs and performance for different certification methods. Different Lyapunov functions require different sampling based on the shape of its level sets. For the MLL Lyapunov function, we sample states in the simplex and reject the states that do not cover the band between the level sets defined by \underline{V} and \bar{V} . For the margin Lyapunov function, we sample on the decision boundary. The more states we sample, the better certified accuracy we could get because the bound with respect to a smaller perturbation is tighter. Number of samples on the decision boundary is an order-of-magnitude smaller than in the simplex, leading to faster certification time and better certified accuracy. Besides the number of samples, another factor that influences the certification time is the way to compute bounds against perturbations. Certifying with Lipschitz bounds is the fastest, since we use orthogonal layers which have Lipschitz constant 1, the certification time is equal to the inference time on all the states. Certifying with CROWN [47] provides the tightest bound but is more computationally expensive than using the Lipschitz bound.

5 Related Works

Empirical Robustness of Neural ODEs. Yan et al. [45] proposes a steady state loss to improve empirical robustness of neural ODEs. A line of work train neural ODEs to stabilize to Lyapunov equilibrium points. Kang et al. [25] adds a regularization term in the loss to encourage the Jacobian of dynamics in neural ODE to have eigenvalues with negative real parts. Huang et al. [22] parametrizes the weights of neural ODE blocks to be skew-symmetric. However, both works only demonstrate empirical robustness improvement from neural ODE but no formal guarantees. Huang et al. [22] also shows that the empirical robustness improvement may be due to the gradient masking effects from the adaptive ODE solvers.

Verification and Certified robustness of Neural ODEs. Previous works on formal analysis of neural ODEs focus on reachability analysis. Stochastic Lagrangian Reachability (SLR) [19] proposes an abstraction-based technique to provide stochastic bound on the reachable set of neural ODEs. Lopez et al. [29] computes deterministic reachable set of neural ODEs via zonotope and polynomial-zonotope

based methods implemented in CORA [2]. However, these methods have only been demonstrated on very low dimension problems or on linear neural ODEs. Another important class of implicit-depth models is monDEQ [41], and it can be thought of as an implicit ODE. There are previous works trying to certify ℓ_2 robustness of monDEQ, either via controlling Lipschitz [31] or semialgebraic representation [10]. However, they do not scale well beyond MNIST.

Formal verification of neural networks. Formal verification of neural networks aim to prove or disprove certain specifications of neural networks, and a canonical problem of neural network verification is to bound the output of neural networks given specified input perturbations. Computing the exact bounds is a NP-complete problem [26] and can be solved via MIP or SMT solvers [36, 17], but they are not scalable and often too expensive for practical usage. In the meanwhile, incomplete neural network verifiers are developed to give sound outer bounds of neural networks [34, 15, 40, 35], and bound-propagation-based methods such as CROWN [47] are a popular approach for incomplete verification. Recently, branch-and-bound based approaches [7, 39, 14] are proposed to further enhance the strength of neural network verifiers. Our work utilizes neural network verifiers as a sub-procedure to prove forward invariance of neural ODEs, and is agnostic to the verification algorithm used. We used CROWN because it is efficient, GPU-accelerated and has high quality implementation [43].

Learning Lyapunov functions and controllers for non-linear control problems. A range of work learns neural network Lyapunov functions [8], barrier functions [24], and control policies [13] for nonlinear control problems. To certify the stability or safety requirements, [8] uses SMT solvers [18], [24] uses Lipschitz methods and [13] formulate the verification as mixed integer programming (MIP). We use a linear relaxation based neural network verifier [47] that enjoys a good balance between tightness and computational cost, enabling us to certify nonlinear control policies ([8, 24] learns linear control policies) on the real dynamics ([13] uses a neural network to approximate the dynamics).

6 Conclusion and Future Work

We have presented FI-ODE: a framework for certified and robust forward invariance of Neural ODEs in both the classification and control contexts. In classification we certify robust forward invariance of the subset of the state-space that produces correct classification by a CBF-QP projection. To improve performance, we explored various sampling schedulers that change the distribution of samples for approximating the Lyapunov Loss during training. Finally, we demonstrate the broad applicability of our methodology by certifying the forward invariance regions of the state-space in a planar segway model.

We consider this a first step towards certification of desirable

properties in complex Neural ODEs for a wide variety of domains from classification to classical control. On the robotics front, our future work includes certifying larger more realistic models robot dynamics. On the learning front, we would like to explore performance improvements for classification using larger and more complex dynamics.

Acknowledgements. This work is funded in part by AeroVironment and NSF #1918865.

References

- [1] A. Agrawal et al. “Differentiable Convex Optimization Layers”. In: *Advances in Neural Information Processing Systems (NeurIPS)*. 2019.
- [2] Matthias Althoff. “Reachability analysis of nonlinear systems using conservative polynomialization and non-convex sets”. In: *Proceedings of the 16th international conference on hybrid systems: computation and control*. 2013, pp. 173–182.
- [3] Aaron D Ames et al. “Control barrier function based quadratic programs for safety critical systems”. In: *IEEE Transactions on Automatic Control* (2016).
- [4] Aaron D Ames et al. “Rapidly exponentially stabilizing control lyapunov functions and hybrid zero dynamics”. In: *IEEE Transactions on Automatic Control* (2014).
- [5] Anish Athalye, Nicholas Carlini, and David A. Wagner. “Obfuscated Gradients Give a False Sense of Security: Circumventing Defenses to Adversarial Examples”. In: *International Conference on Machine Learning (ICML)*. 2018.
- [6] Akhilan Boopathy et al. “Fast Training of Provably Robust Neural Networks by SingleProp”. In: *Proceedings of the AAAI Conference on Artificial Intelligence*. 2021.
- [7] Rudy Bunel et al. “Branch and bound for piecewise linear neural network verification”. In: *Journal of Machine Learning Research (JMLR)* (2020).
- [8] Ya-Chien Chang, Nima Roohi, and Sicun Gao. “Neural lyapunov control”. In: *Advances in Neural Information Processing Systems (NeurIPS)* 32 (2019).
- [9] Ricky TQ Chen et al. “Neural ordinary differential equations”. In: *Advances in Neural Information Processing Systems (NeurIPS)* (2018).
- [10] Tong Chen et al. “Semialgebraic representation of monotone deep equilibrium models and applications to certification”. In: *Advances in Neural Information Processing Systems (NeurIPS)* 34 (2021), pp. 27146–27159.
- [11] Jeremy Cohen, Elan Rosenfeld, and Zico Kolter. “Certified adversarial robustness via randomized smoothing”. In: *International Conference on Machine Learning (ICML)*. 2019.
- [12] Francesco Croce and Matthias Hein. “Reliable evaluation of adversarial robustness with an ensemble of diverse parameter-free attacks”. In: *International Conference on Machine Learning (ICML)*. PMLR. 2020, pp. 2206–2216.
- [13] Hongkai Dai et al. “Lyapunov-stable neural-network control”. In: *Robotics: Science and Systems (RSS)* (2021).
- [14] Alessandro De Palma et al. “Scaling the Convex Barrier with Active Sets”. In: *International Conference on Learning Representations (ICLR)* (2021).
- [15] Krishnamurthy Dvijotham et al. “A dual approach to scalable verification of deep networks”. In: *Conference on Uncertainty in Artificial Intelligence (UAI)* (2018).
- [16] Weinan E. “A proposal on machine learning via dynamical systems”. In: *Communications in Mathematics and Statistics* 5.1 (2017), pp. 1–11.
- [17] Ruediger Ehlers. “Formal verification of piece-wise linear feed-forward neural networks”. In: *International Symposium on Automated Technology for Verification and Analysis (ATVA)*. 2017.
- [18] Sicun Gao, Soonho Kong, and Edmund M Clarke. “dReal: An SMT solver for nonlinear theories over the reals”. In: *International conference on automated deduction*. Springer. 2013, pp. 208–214.
- [19] Sophie Grunbacher et al. “On the verification of neural odes with stochastic guarantees”. In: *Proceedings of the AAAI Conference on Artificial Intelligence*. 2021.
- [20] Thomas Gurriet et al. “Towards a framework for realizable safety critical control through active set invariance”. In: *2018 ACM/IEEE 9th International Conference on Cyber-Physical Systems (ICCPS)*. IEEE. 2018.
- [21] Eldad Haber and Lars Ruthotto. “Stable architectures for deep neural networks”. In: *Inverse Problems* 34.1 (Dec. 2017), p. 014004.
- [22] Yifei Huang et al. “Adversarial Robustness of Stabilized Neural ODE Might be from Obfuscated Gradients”. In: *Mathematical and Scientific Machine Learning*. PMLR. 2022.
- [23] Ivan Dario Jimenez Rodriguez, Aaron D Ames, and Yisong Yue. “LyaNet: A Lyapunov Framework for Training Neural ODEs”. In: *International Conference on Machine Learning (ICML)*. 2022.
- [24] Wanxin Jin et al. “Neural certificates for safe control policies”. In: *arXiv preprint arXiv:2006.08465* (2020).
- [25] Qiyu Kang et al. “Stable Neural ODE with Lyapunov-Stable Equilibrium Points for Defending Against Adversarial Attacks”. In: *Advances in Neural Information Processing Systems (NeurIPS)* (2021).

- [26] Guy Katz et al. “Reluplex: An efficient SMT solver for verifying deep neural networks”. In: *International Conference on Computer Aided Verification (CAV)*. 2017.
- [27] Islam Khalil, JC Doyle, and K Glover. *Robust and optimal control*. prentice hall, new jersey, 1996.
- [28] Xuanqing Liu et al. “How does noise help robustness? explanation and exploration under the neural sde framework”. In: *Proceedings of the IEEE/CVF Conference on Computer Vision and Pattern Recognition (CVPR)*. 2020, pp. 282–290.
- [29] Diego Manzananas Lopez et al. “Reachability Analysis of a General Class of Neural Ordinary Differential Equations”. In: *arXiv preprint arXiv:2207.06531* (2022).
- [30] Mitio Nagumo. “Über die lage der integralkurven gewöhnlicher differentialgleichungen”. In: *Proceedings of the Physico-Mathematical Society of Japan. 3rd Series* (1942).
- [31] Chirag Pabbaraju, Ezra Winston, and J Zico Kolter. “Estimating Lipschitz constants of monotone deep equilibrium models”. In: *International Conference on Learning Representations (ICLR)*. 2020.
- [32] Aditi Raghunathan, Jacob Steinhardt, and Percy Liang. “Certified defenses against adversarial examples”. In: *International Conference on Learning Representations (ICLR)*. 2018.
- [33] Ivan Dario Jimenez Rodriguez et al. “Neural Gaits: Learning Bipedal Locomotion via Control Barrier Functions and Zero Dynamics Policies”. In: *Conference on Learning for Dynamics and Control (LADC)* (2022).
- [34] Hadi Salman et al. “A Convex Relaxation Barrier to Tight Robustness Verification of Neural Networks”. In: *Advances in Neural Information Processing Systems (NeurIPS)*. 2019.
- [35] Gagandeep Singh et al. “An abstract domain for certifying neural networks”. In: *Proceedings of the ACM on Programming Languages (POPL)* (2019).
- [36] Vincent Tjeng, Kai Xiao, and Russ Tedrake. “Evaluating Robustness of Neural Networks with Mixed Integer Programming”. In: *International Conference on Learning Representations (ICLR)* (2019).
- [37] Asher Trockman and J Zico Kolter. “Orthogonalizing convolutional layers with the cayley transform”. In: *International Conference on Learning Representations (ICLR)* (2021).
- [38] Yusuke Tsuzuku, Issei Sato, and Masashi Sugiyama. “Lipschitz-Margin Training: Scalable Certification of Perturbation Invariance for Deep Neural Networks”. In: *Advances in Neural Information Processing Systems (NeurIPS)*. 2018.
- [39] Shiqi Wang et al. “Beta-crown: Efficient bound propagation with per-neuron split constraints for neural network robustness verification”. In: *Advances in Neural Information Processing Systems (NeurIPS)* (2021).
- [40] Shiqi Wang et al. “Efficient formal safety analysis of neural networks”. In: *Advances in Neural Information Processing Systems (NeurIPS)*. 2018.
- [41] Ezra Winston and J Zico Kolter. “Monotone operator equilibrium networks”. In: *Advances in Neural Information Processing Systems (NeurIPS)* 33 (2020), pp. 10718–10728.
- [42] Eric Wong and J. Zico Kolter. “Provable Defenses against Adversarial Examples via the Convex Outer Adversarial Polytope”. In: *International Conference on Machine Learning (ICML)*. 2018.
- [43] Kaidi Xu et al. “Automatic Perturbation Analysis for Scalable Certified Robustness and Beyond”. In: *Advances in Neural Information Processing Systems (NeurIPS)* (2020).
- [44] Xiangru Xu et al. “Robustness of control barrier functions for safety critical control”. In: *IFAC-PapersOnLine* (2015).
- [45] Hanshu Yan et al. “On robustness of neural ordinary differential equations”. In: *International Conference on Learning Representations (ICLR)* (2020).
- [46] Anna Yershova and Steven M LaValle. “Deterministic sampling methods for spheres and SO (3)”. In: *IEEE International Conference on Robotics and Automation, 2004. Proceedings. ICRA'04. 2004*. 2004.
- [47] Huan Zhang et al. “Efficient neural network robustness certification with general activation functions”. In: *Advances in Neural Information Processing Systems (NeurIPS)* 31 (2018).

Supplementary Material

A Definitions

A.1 Class \mathcal{K} functions

Definition 4 (Class \mathcal{K} Function). A continuous function $\alpha : [0, a) \rightarrow [0, \infty)$ for $a \in \mathbb{R}_{>0} \cup \{\infty\}$ belongs to class \mathcal{K} ($a \in \mathcal{K}$) if it satisfies:

1. **Zero at Zero:** $\alpha(0) = 0$
2. **Strictly Increasing:** For all $r_1, r_2 \in [0, a]$ we have that $r_1 < r_2 \Rightarrow \alpha(r_1) < \alpha(r_2)$

Definition 5 (Class \mathcal{K}_∞ Function). A function belongs to \mathcal{K}_∞ if it satisfies:

1. $\alpha \in \mathcal{K}$
2. **Radially Unbounded:** $\lim_{r \rightarrow \infty} \alpha(r) = \infty$

Definition 6 (Extended Class \mathcal{K}_∞^e Function). A continuous function $\alpha : \mathbb{R} \rightarrow \mathbb{R}$ belongs to extended \mathcal{K}_∞^e if it satisfies:

1. **Zero at Zero:** $\alpha(0) = 0$
2. **Strictly Increasing:** For all $r_1, r_2 \in [0, a]$ we have that $r_1 < r_2 \Rightarrow \alpha(r_1) < \alpha(r_2)$

A.2 Barrier Loss

Recall that $\boldsymbol{\eta} \in \mathcal{H} \subset \mathbb{R}^k$. Suppose we wish to render the set $\mathcal{S} = \{\boldsymbol{\eta} \in \mathcal{H} : h(\boldsymbol{\eta}) \geq 0\}$ where $h : \mathcal{H} \rightarrow \mathbb{R}$ is a continuously differentiable function. Systems that satisfy barrier conditions in Theorem 2.2 provides two properties: forward invariance of \mathcal{S} and stability of the system towards \mathcal{S} . This stability can be local to a subset of the state-space that contains the desired set. Namely, we expect the property $\mathcal{S} \subseteq \mathcal{R} \subseteq \mathcal{H}$ where \mathcal{R} is the region of attraction. With this added detail to the problem setting we are ready to state the definition of Barrier loss:

Definition 7 (Barrier Loss). For a barrier function candidate $h : \mathcal{H} \rightarrow \mathbb{R}$, with function $\alpha \in \mathcal{K}_\infty^e$ and its corresponding region of attraction \mathcal{R} , the Barrier Loss $\mathcal{L} : \boldsymbol{\Theta} \rightarrow \mathbb{R}_{\geq 0}$ is defined as:

$$\mathcal{L}(\boldsymbol{\theta}) = \int_{\mathcal{R} \times [0, 1]} \max\{0, -\frac{\partial h^\top}{\partial \boldsymbol{\eta}} \mathbf{f}_{\boldsymbol{\theta}}(\boldsymbol{\eta}, \mathbf{x}, t) - \alpha(h(\boldsymbol{\eta}))\} d\boldsymbol{\eta} \times t \quad (15)$$

B PROOFS

B.1 Proof of Theorem 3.1

Proof. First, we prove that evolving the perturbed system for sufficient integration time guarantees that $V(\boldsymbol{\eta}(T)) \leq \underline{V}$. Then, we prove that $\mathcal{C} = \{\boldsymbol{\eta} \in \Delta \mid V(\boldsymbol{\eta}) \leq \underline{V}\}$ is a forward invariant set for the perturbed system.

Suppose $\boldsymbol{\eta} \in \Omega_{\overline{V} \setminus \underline{V}}$. Then we have

$$\dot{V}(\boldsymbol{\eta}, \mathbf{x} + \boldsymbol{\epsilon}) = \frac{\partial V^\top}{\partial \boldsymbol{\eta}} \mathbf{f}(\boldsymbol{\eta}, \mathbf{x} + \boldsymbol{\epsilon}, t) \quad (16)$$

$$= \frac{\partial V^\top}{\partial \boldsymbol{\eta}} \mathbf{f}(\boldsymbol{\eta}, \mathbf{x}, t) + \frac{\partial V^\top}{\partial \boldsymbol{\eta}} \mathbf{f}(\boldsymbol{\eta}, \mathbf{x} + \boldsymbol{\epsilon}, t) - \frac{\partial V^\top}{\partial \boldsymbol{\eta}} \mathbf{f}(\boldsymbol{\eta}, \mathbf{x}, t) \quad (17)$$

$$\leq -\kappa V(\boldsymbol{\eta}) + L_V L_f^x \bar{\epsilon} \quad (18)$$

Where the last line follows from our assumption of ES-CLF on the nominal system and Cauchy-Schwarz. Notice that for this bound must apply everywhere in $\Omega_{\bar{V} \setminus \underline{V}}$ it is sufficient to show that it applies for \underline{V} . This last condition is true by the **Sufficient Exponential Stability** assumption. By direct application of the comparison lemma as shown in the appendix of [23], we can obtain the following bound:

$$V(\boldsymbol{\eta}(t; \mathbf{x} + \boldsymbol{\epsilon})) \leq V(\boldsymbol{\eta}(0))e^{-\kappa t} + \frac{L_V L_f^x \bar{\epsilon}}{\kappa}(1 - e^{-\kappa t}) \quad (19)$$

Now we need to solve for the integration time required to ensure correct classification. Since we know \underline{V} implies correct classification, it is sufficient to solve for the time that ensures we cross this level set:

$$V(\boldsymbol{\eta}(0))e^{-\kappa t} + \frac{L_V L_f^x \bar{\epsilon}}{\kappa}(1 - e^{-\kappa t}) \leq \underline{V} \quad (20)$$

which gives us

$$t \geq -\frac{1}{\kappa} \log \frac{\underline{V} - \frac{L_V L_f^x \bar{\epsilon}}{\kappa}}{V(\boldsymbol{\eta}(0)) - \frac{L_V L_f^x \bar{\epsilon}}{\kappa}} \quad (21)$$

Therefore by the comparison lemma, since we have **sufficient exponential stability**, evolving the perturbed system for **sufficient integration time** guarantees $V(\boldsymbol{\eta}(T)) \leq \underline{V}$.

Define barrier function as $h = \underline{V} - V$, then \mathcal{S} is a 0-superlevel set of h . According to Nagumo's theorem, if $\dot{h}(\mathbf{x} + \boldsymbol{\epsilon}; \boldsymbol{\eta}) \geq 0$ on $\partial\mathcal{S} = \{\boldsymbol{\eta} \in \Delta | V(\boldsymbol{\eta}) = \underline{V}\}$, then \mathcal{S} is forward invariant. Since $\dot{V}(\boldsymbol{\eta}; \mathbf{x}) \leq -\kappa V$ on $\Omega_{\bar{V} \setminus \underline{V}}$, we have $\dot{h}(\boldsymbol{\eta}; \mathbf{x}) \geq \kappa \underline{V}$ on $\partial\mathcal{S}$. Then for perturbed input, we have

$$\begin{aligned} \dot{h}(\boldsymbol{\eta}; \mathbf{x} + \boldsymbol{\epsilon}) &= \dot{h}(\boldsymbol{\eta}; \mathbf{x}) + \dot{h}(\boldsymbol{\eta}; \mathbf{x} + \boldsymbol{\epsilon}) - \dot{h}(\boldsymbol{\eta}; \mathbf{x}) \\ &\geq \dot{h}(\boldsymbol{\eta}; \mathbf{x}) - L_h L_f^x \bar{\epsilon} \geq \kappa \underline{V} - L_h L_f^x \bar{\epsilon} \geq 0 \end{aligned} \quad (22)$$

□

B.2 Proof of Theorem 3.2 (a)

Proof. For any $\boldsymbol{\eta} \in \Delta$, let $\mathbf{s}^0 = [T\boldsymbol{\eta}_1, \dots, T\boldsymbol{\eta}_n]$, then by definition of the simplex, we have $\sum_i \mathbf{s}_i^0 = T$. Let $\mathbf{s}^1 = [\lceil \boldsymbol{\eta}_1 T \rceil, \dots, \lceil \boldsymbol{\eta}_n T \rceil]$, and $\mathbf{s}^2 = [\lfloor \boldsymbol{\eta}_1 T \rfloor, \dots, \lfloor \boldsymbol{\eta}_n T \rfloor]$. We have $0 \leq \sum_i (\mathbf{s}_i^1 - \mathbf{s}_i^0) < n$, $|\mathbf{s}_i^0 - \mathbf{s}_i^1| < 1$, and $|\mathbf{s}_i^0 - \mathbf{s}_i^2| < 1$. Define $m = \sum_i (\mathbf{s}_i^1 - \mathbf{s}_i^0)$, then there exists $M \geq m$ elements in \mathbf{s}^1 such that $\mathbf{s}_i^1 > \mathbf{s}_i^0 > \mathbf{s}_i^2 \geq 0$ (otherwise $\sum_i (\mathbf{s}_i^1 - \mathbf{s}_i^0) < m$). Let the indices of such elements be i_1, \dots, i_M , and let \mathcal{I} be the set that contains the first m indices: $\mathcal{I} = \{i_1, \dots, i_m\}$. We construct \mathbf{s}^* as the following so that $\mathbf{s}^* \in S$:

$$\mathbf{s}_i^* = \begin{cases} \mathbf{s}_i^2, & i \in \mathcal{I} \\ \mathbf{s}_i^1, & \text{otherwise} \end{cases} \quad (23)$$

Check that $\sum_i \mathbf{s}_i^* = \sum_i \mathbf{s}_i^1 - m = T$, $\mathbf{s}_i^* \geq 0$, and $|T\boldsymbol{\eta}_i - \mathbf{s}_i^*| < 1$. Therefore, for any $\boldsymbol{\eta} \in \Delta$, there exists $\mathbf{s}^* \in S$ such that $|T\boldsymbol{\eta}_i - \mathbf{s}_i^*| < 1$. □

B.3 Proof of Theorem 3.2 (b)

Proof. For any $\boldsymbol{\eta} \in \mathcal{D}_y$, let $\mathbf{z} = [T\boldsymbol{\eta}_1, \dots, T\boldsymbol{\eta}_n]$. By definition of \mathcal{D}_y , in addition to $\sum_i \mathbf{z}_i = T$, we have

$$\sum_i \mathbf{z}_i = T \quad (24)$$

$$\mathbf{z}_y = \max_{j \neq y} \mathbf{z}_j \quad (25)$$

Define $\tilde{\mathbf{z}} = [\mathbf{z}_1 - \lfloor \mathbf{z}_1 \rfloor, \dots, \mathbf{z}_n - \lfloor \mathbf{z}_n \rfloor]$ to be the vector that contains the fractional part of each element in \mathbf{z} . Then we sort $\tilde{\mathbf{z}}$ in a non-decreasing order. For the tied elements that equals to $\tilde{\mathbf{z}}_y$, we put $\tilde{\mathbf{z}}_y$ as the last. We denote the sorted vector as $\tilde{\mathbf{z}}' = [\tilde{\mathbf{z}}_{i_1}, \dots, \tilde{\mathbf{z}}_{i_n}]$, where $\tilde{\mathbf{z}}_{i_1} \leq \dots \leq \tilde{\mathbf{z}}_{i_n}$. Let $v : \mathbb{Z}^+ \rightarrow \mathbb{Z}^+$ to be a function that maps the indices in $\tilde{\mathbf{z}}$ to the indices in $\tilde{\mathbf{z}}'$. For instance, if $\tilde{\mathbf{z}}_1$ becomes the third element in $\tilde{\mathbf{z}}'$, then $v(1) = 3$. If $\tilde{\mathbf{z}}_j = \tilde{\mathbf{z}}_y$, we have $v(j) > v(j)$.

Notice that $\sum_i \tilde{z}'_i = \sum_i \tilde{z}_i = \sum_i z_i - \sum_i \lfloor z_i \rfloor = T - \sum_i \lfloor z_i \rfloor$, and $\sum_i \tilde{z}'_i < n$ since $0 \leq \tilde{z}'_i < 1$ for $i = 1, \dots, n$. Let $k = n - (T - \sum_i \lfloor z_i \rfloor)$, we have

$$\tilde{z}'_1 + \dots + \tilde{z}'_k = (1 - \tilde{z}'_{k+1}) + \dots + (1 - \tilde{z}'_n) \quad (26)$$

Define vector \mathbf{q} as follows:

$$\mathbf{q}_{i_j} = \begin{cases} \lfloor T\eta_{i_j} \rfloor, & j = 1, \dots, k \\ \lceil T\eta_{i_j} \rceil, & j = k+1, \dots, n \end{cases} \quad (27)$$

Then we have $|\mathbf{q}_i - z_i| < 1$ for all $i = 1, \dots, n$. Now we check \mathbf{q} satisfies Equation (24) and a relaxed version of Equation (25). First, we have $\sum_i \mathbf{q}_i = T$ because of Equation (26). Next, we show $\mathbf{q}_y \geq \max_{i \neq y} \mathbf{q}_i$ by contradiction. Suppose there exists an index j such that $\mathbf{q}_j > \mathbf{q}_y$, then it has to be the case where $\lfloor z_j \rfloor = \lfloor z_y \rfloor$ and we take ceiling on z_j and take floor on z_y , i.e. $v(j) > k$ and $v(y) \leq k$. This means $\tilde{z}_j > \tilde{z}_y$, because v is the sorted indices of \tilde{z} in a non-decreasing order and this gives $\tilde{z}_j \geq \tilde{z}_y$, and if $\tilde{z}_j = \tilde{z}_y$, we have $v(y) > v(j)$, which is contradictory to $v(j) > k$ and $v(y) \leq k$. Then we have $z_y = \lfloor z_y \rfloor + \tilde{z}_y < z_j = \lfloor z_j \rfloor + \tilde{z}_j$, which is contradictory to Equation (25). Therefore, there does not exist a j such that $\mathbf{q}_j > \mathbf{q}_y$, i.e. $\mathbf{q}_y \geq \max_{i \neq y} \mathbf{q}_i$. For the cases where $\mathbf{q}_y = \max_{i \neq y} \mathbf{q}_i$, we have $\mathbf{q} \in S_y$, i.e. \mathbf{q} is a sampled point.

For the cases where $\mathbf{q}_y > \max_{i \neq y} \mathbf{q}_i$, we show that we can modify \mathbf{q} to $\tilde{\mathbf{q}}$ such that $\tilde{\mathbf{q}} \in S_y$ and $|\tilde{\mathbf{q}}_i - z_i| \leq 1$ for all $i = 1, \dots, n$. Let $\mathcal{I} = \{i \in \mathbb{Z}^+ | z_i \neq y, z_i = z_y\}$ be the set that contains the indices of all runner-up elements in z . If $\mathbf{q}_y > \max_{i \neq y} \mathbf{q}_i$, then we must have $\mathbf{q}_y = \lceil T\eta_y \rceil$, and $\mathbf{q}_i = \lfloor T\eta_i \rfloor$ for all $i \in \mathcal{I}$. We first let $\tilde{\mathbf{q}} = \mathbf{q}$, and then pick an i^* from \mathcal{I} . Let $\mathcal{J} = \{j \in \mathbb{Z}^+ | \mathbf{q}_j \geq 1, j \neq i^*, j \neq y\}$. Notice that $\mathbf{q}_{i^*} + \mathbf{q}_y = 2\lfloor z_y \rfloor + 1$, which is an odd number. Since $\sum_i \mathbf{q}_i = T$ and T is an even number, $\mathcal{J} \neq \emptyset$. We discuss how to obtain $\tilde{\mathbf{q}}$ case by case.

Case 1: If there exists a $j \in \mathcal{J}$ such that $v(j) > k$, we set $\tilde{\mathbf{q}}_j = \lfloor T\eta_j \rfloor$, and set $\tilde{\mathbf{q}}_{i^*} = \lceil T\eta_{i^*} \rceil$. Then we have $\sum_i \tilde{\mathbf{q}}_i = \sum_{i \neq i^*, i \neq j} \mathbf{q}_i + \mathbf{q}_{i^*} + 1 + \mathbf{q}_j - 1 = T$ and $|\tilde{\mathbf{q}}_i - z_i| \leq 1$ for all $i = 1, \dots, n$.

Case 2: If $v(j) \leq k$ for all $j \in \mathcal{J}$, there must exist a j such that $\mathbf{q}_j < \mathbf{q}_{i^*}$. Otherwise, $\mathbf{q}_y = \mathbf{q}_{i^*} + 1$, and $\mathbf{q}_i = \mathbf{q}_{i^*}$ for all $i \neq y$. Then $\sum_i \mathbf{q}_i = T = n\mathbf{q}_{i^*} + 1$, which is contradictory to the assumption that $T \not\equiv 1 \pmod{n}$. Then set $\tilde{\mathbf{q}}_j = \lceil T\eta_j \rceil$ and $\tilde{\mathbf{q}}_y = \lfloor T\eta_y \rfloor$. Since $\mathbf{q}_j < \mathbf{q}_{i^*}$, we have $\tilde{\mathbf{q}}_j = \mathbf{q}_j + 1 \leq \tilde{\mathbf{q}}_y = \mathbf{q}_{i^*}$. \square

Remark. The assumption that $T \not\equiv 1 \pmod{n}$ is easy to satisfy. Since we also require T is an even number, as long as n is also an even number, we have $T \not\equiv 1 \pmod{n}$. We can also relax this assumption by adding $[\frac{T}{n}, \dots, \frac{T}{n}]$ to S_y .

B.4 Custom solver for the CBF-QP

Consider a CBF-QP in the following form:

$$\begin{aligned} f(\hat{\mathbf{f}}) &= \underset{\mathbf{f} \in \mathbb{R}^n}{\operatorname{argmin}} \frac{1}{2} \|\mathbf{f} - \hat{\mathbf{f}}\|_2^2 \\ \text{s.t.} \quad & \mathbb{1}^\top \mathbf{f} = b \\ & \underline{\mathbf{f}}(\boldsymbol{\eta}) \leq \mathbf{f} \leq \bar{\mathbf{f}}(\boldsymbol{\eta}) \end{aligned} \quad (28)$$

where $\underline{\mathbf{f}}$ and $\bar{\mathbf{f}}$ are non-increasing function of $\boldsymbol{\eta}$. By the Karush–Kuhn–Tucker (KKT) conditions, the solution of (28) is as follows:

$$f(\hat{\mathbf{f}}) = \left[\hat{\mathbf{f}} + \lambda^* \mathbb{1} \right]_{\underline{\mathbf{f}}}^{\bar{\mathbf{f}}} \quad (29)$$

where $[\cdot]_{\underline{\mathbf{f}}}^{\bar{\mathbf{f}}}$ stands for lower and upper clipping by $\underline{\mathbf{f}}$ and $\bar{\mathbf{f}}$, and λ^* is the Lagrangian multiplier. We find λ^* such that $\mathbb{1}^\top f(\hat{\mathbf{f}}) = b$ using binary search. Since $f(\hat{\mathbf{f}})$ is clipped by $\underline{\mathbf{f}}$ and $\bar{\mathbf{f}}$, the search range of λ^* is $[\min_i (f_i - \underline{f}_i), \max_i (\bar{f}_i - f_i)]$, where f_i stands for the i th element in $f(\hat{\mathbf{f}})$, and $\underline{f}_i, \bar{f}_i$ stand for the i th element in $\underline{\mathbf{f}}(\boldsymbol{\eta})$ and $\bar{\mathbf{f}}(\boldsymbol{\eta})$ respectively.

To differentiate through the solver in training, we derive the derivatives based on the binding conditions of the inequality constraints. First, we define the binding and not binding sets as follows:

$$S = \{i | f_i = \underline{f}_i \text{ or } f_i = \bar{f}_i\}, \quad S^c = \Omega \setminus S \quad (30)$$

$$S_l = \{i | f_i = \underline{f}_i\}, \quad S_l^c = \Omega \setminus S_l \quad (31)$$

$$S_u = \{i | f_i = \bar{f}_i\}, \quad S_u^c = \Omega \setminus S_u \quad (32)$$

where $\Omega = \{i \in \mathbb{Z}^+ | i \leq n\}$. Then the derivatives of f with respect to the inputs $\hat{\mathbf{f}}$, $\underline{\mathbf{f}}$ and $\overline{\mathbf{f}}$ are as follows:

$$\frac{df_i}{d\hat{\mathbf{f}}_j} = \begin{cases} 0, & i \in \mathcal{S}^c \text{ or } j \in \mathcal{S}^c \\ 1 - \frac{1}{n(\mathcal{S})}, & i = j \in \mathcal{S} \\ -\frac{1}{n(\mathcal{S})}, & i \neq j, i \in \mathcal{S}, j \in \mathcal{S} \end{cases} \quad (33)$$

$$\frac{df_i}{d\underline{\mathbf{f}}_j} = \begin{cases} 0, & j \in \mathcal{S}_l, \forall i \in \Omega \\ 0, & j \in \mathcal{S}_l^c, i \in \mathcal{S}_l^c \setminus \{j\} \\ 1, & j \in \mathcal{S}_l^c, i = j \\ -\frac{1}{n(\mathcal{S}_l)}, & j \in \mathcal{S}_l^c, i \in \mathcal{S}_l \end{cases} \quad \frac{df_i}{d\overline{\mathbf{f}}_j} = \begin{cases} 0, & j \in \mathcal{S}_u, \forall i \in \Omega \\ 0, & j \in \mathcal{S}_u^c, i \in \mathcal{S}_u^c \setminus \{j\} \\ 1, & j \in \mathcal{S}_u^c, i = j \\ -\frac{1}{n(\mathcal{S}_u)}, & j \in \mathcal{S}_u^c, i \in \mathcal{S}_u \end{cases} \quad (34)$$

B.5 Interval Bound Propagation through CBF-QP

Proposition B.1. Consider a CBF-QP in the form of 28. Define function h_i to be $h_i : \boldsymbol{\eta}, \hat{\mathbf{f}} \mapsto f(\hat{\mathbf{f}})_i$. Given perturbed input in an interval bound $\underline{\hat{\mathbf{f}}}_i \leq \hat{\mathbf{f}}_i \leq \overline{\hat{\mathbf{f}}}_i$, and $\underline{\boldsymbol{\eta}}_i \leq \boldsymbol{\eta}_i \leq \overline{\boldsymbol{\eta}}_i$, we have

$$h_i(\boldsymbol{\eta}_{ub}^i, \hat{\mathbf{f}}_{lb}^i) \leq f(\hat{\mathbf{f}})_i \leq h_i(\boldsymbol{\eta}_{lb}^i, \hat{\mathbf{f}}_{ub}^i) \quad (35)$$

where $\boldsymbol{\eta}_{ub}^i, \boldsymbol{\eta}_{lb}^i$ are defined as follows and $\hat{\mathbf{f}}_{ub}^i, \hat{\mathbf{f}}_{lb}^i$ are defined similarly:

$$\boldsymbol{\eta}_{ub}^i = \begin{cases} \overline{\boldsymbol{\eta}}_j, & j = i \\ \underline{\boldsymbol{\eta}}_j, & j \neq i \end{cases} \quad \boldsymbol{\eta}_{lb}^i = \begin{cases} \underline{\boldsymbol{\eta}}_j, & j = i \\ \overline{\boldsymbol{\eta}}_j, & j \neq i \end{cases} \quad (36)$$

Proof. We prove by contradiction. For the upper bound $f(\hat{\mathbf{f}})_i \leq h_i(\boldsymbol{\eta}_{lb}^i, \hat{\mathbf{f}}_{ub}^i)$, suppose $f(\hat{\mathbf{f}})_i > h_i(\boldsymbol{\eta}_{lb}^i, \hat{\mathbf{f}}_{ub}^i)$. Plug in Equation (29), we have

$$\left[\hat{\mathbf{f}}_i + \lambda \right]_{\underline{\mathbf{f}}(\boldsymbol{\eta}_i)}^{\overline{\mathbf{f}}(\boldsymbol{\eta}_i)} > \left[\hat{\mathbf{f}}_i + \lambda' \right]_{\underline{\mathbf{f}}(\boldsymbol{\eta}_i)}^{\overline{\mathbf{f}}(\boldsymbol{\eta}_i)} \quad (37)$$

Since $\underline{\mathbf{f}}$ and $\overline{\mathbf{f}}$ are non-increasing function of $\boldsymbol{\eta}$, we have $\underline{\mathbf{f}}(\overline{\boldsymbol{\eta}}_i) \geq \underline{\mathbf{f}}(\boldsymbol{\eta}_i)$ and $\overline{\mathbf{f}}(\underline{\boldsymbol{\eta}}_i) \geq \overline{\mathbf{f}}(\boldsymbol{\eta}_i)$. Then $\hat{\mathbf{f}}_i + \lambda > \hat{\mathbf{f}}_i + \lambda'$. Since $\hat{\mathbf{f}}_i \leq \overline{\hat{\mathbf{f}}}_i$, we have $\lambda > \lambda'$. Then for all $j \neq i$, we have

$$\left[\hat{\mathbf{f}}_j + \lambda \right]_{\underline{\mathbf{f}}(\boldsymbol{\eta}_j)}^{\overline{\mathbf{f}}(\boldsymbol{\eta}_j)} \geq \left[\hat{\mathbf{f}}_j + \lambda' \right]_{\underline{\mathbf{f}}(\boldsymbol{\eta}_j)}^{\overline{\mathbf{f}}(\boldsymbol{\eta}_j)} \quad (38)$$

Sum on both sides of 37 and 38, we have

$$\mathbb{1}^\top f(\boldsymbol{\eta}, \hat{\mathbf{f}}) > \mathbb{1}^\top f(\boldsymbol{\eta}_{lb}, \hat{\mathbf{f}}_{ub}) \quad (39)$$

which is contradictory to the equality constraint in 28. Therefore, we have $f(\hat{\mathbf{f}})_i \leq h_i(\boldsymbol{\eta}_{lb}^i, \hat{\mathbf{f}}_{ub}^i)$. The lower bound in 35 can be proved in a similar way. \square

C SAMPLING ALGORITHMS

C.1 Sampling on the decision boundary

We describe the process of generating samples on the decision boundary in Algorithm 2. The trick is to break down the n -class decision boundary sampling problem to 2 to $(n-1)$ -class sampling problems. For instance, to generate samples with k non-zero elements on an n -class decision boundary with density T , one can sample points on an k -class decision boundary with density $T-k$ first, adding 1 to each dimension to make each element non-zero, and assign each element to an n dimensional vector. This operation is denoted by function G in Algorithm 2. G takes two list inputs a and c , increases each element in a by 1, rearranges the elements in a according to the indices given by c , and output a new list w of shape k . Equation 40 gives the form of the output of G . If the inputs are $y=0, a=(3,2,3,0), c=\{2,3,7\}$ and $k=8$ (y is the label, a corresponds to a point on 4-class decision boundary, and c specifies the non-zero dimension except for the label dimension in an 8 dimensional vector), then the output is $w=(4,0,3,4,0,0,0,1)$.

$$w_i = \begin{cases} a_0 + 1, & i = y \\ a_{|\{1,2,\dots,i\} \cap c|} + 1, & i \in c \\ 0, & \text{o/w} \end{cases} \quad (40)$$

Algorithm 2: Sample the points on the decision boundary by dynamic programming.

Input : Number of classes K , sample density T , solution set sol with dimension $T \times K$.

// Initialize sol .

Initialize each element of sol to be \emptyset .

$\text{sol}[0][k] = \{\mathbf{0}_k\}$, where $\mathbf{0}_k = [0, \dots, 0] \in \mathbb{R}^k$.

$\text{sol}[j][2] = \{[j/2, j/2]\}$.

// Append elements to $\text{sol}[j][k]$.

for j from 2 to T **do**

for k from 3 to K **do**

for l from 0 to $k - 2$ **do**

if $j - k + l \geq 0$ and $k - l \geq 0$ **then**

 Let \mathcal{C} be the set that contains $k - l - 1$ combinations of $\{1, 2, \dots, k - 1\}$.

$\text{sol}[j][k] = \text{sol}[j][k] \cup \{G(y, a, c, k) | a \in \text{sol}[j - k + l][k - l], c \in \mathcal{C}\}$.

return $\tilde{S}_y = \text{sol}[T][K]/T$

C.2 Rejection sampling

Mathematically, define the distance between two sets S_1, S_2 as $d(S_1, S_2) = \inf\{\|x - y\|_2 | x \in S_1, y \in S_2\}$. Let h be the barrier function, $L_0 = \{\boldsymbol{\eta} | h(\boldsymbol{\eta}) = 0\}$ be the 0-level set, and L_1, L_2 be the c_1 -level set and c_2 -level set that surrounds L_0 , where $c_1 < 0 < c_2$. First, we sample mesh grids in a hypercube with fixed interval r along each dimension. Then we find c_1 and c_2 such that $d(L_1, L_0) \geq \frac{\sqrt{n}}{2}r$ and $d(L_2, L_0) \geq \frac{\sqrt{n}}{2}r$. Since the sampling interval is r , given a point $\boldsymbol{\eta} \in L_0$, there exists a point $\boldsymbol{\eta}^*$ from the mesh grids such that $|\boldsymbol{\eta}_i - \boldsymbol{\eta}_i^*| \leq \frac{r}{2}$ and $c_1 < h(\boldsymbol{\eta}^*) < c_2$. Therefore, we reject points with barrier function values less than c_1 or greater than c_2 and verify the Lyapunov condition holds around a hypercube with side length r for the mesh grids between L_1 and L_2 . If the verification passes, the Lyapunov condition holds everywhere on L_0 .

D EXPERIMENT DETAILS

D.1 Image classification

To restrict the Lipschitz of the dynamics, we use orthogonal layers [37] in the neural network. Specifically, we have $\hat{\mathbf{f}}(\boldsymbol{\eta}, x) = W_3\sigma(W_2\sigma(W_1\boldsymbol{\eta} + g(x)) + b_2) + b_3$, where g is a neural network with 4 orthogonal convolution layers and 3 orthogonal linear layers, and W_1, W_2, W_3 are orthogonal matrices, σ is the ReLU activation function.

In the CBF-QP, we need to pick a class \mathcal{K}_∞^e function α for the inequality constraint $\mathbf{f} \geq -\alpha(\boldsymbol{\eta})$. Here we use $\alpha(\boldsymbol{\eta}) = c_1(e^{c_2\boldsymbol{\eta}} - 1)$, where $c_1 = 100$, and $c_2 = 0.02$. Comparing with a linear function, this $\alpha(\boldsymbol{\eta})$ leads to a higher margin over Lipschitz ratio, resulting in better certified accuracy.

For certification, we choose $T = 40$ when sampling on the decision boundary. A larger T will lead to better certified accuracy but increases the computational cost dramatically. We ran the experiments on an NVIDIA RTX A6000 GPU.

D.2 Nonlinear control

The dynamics for the segway system is:

$$\frac{d}{dt} \begin{bmatrix} \phi \\ v \\ \dot{\phi} \end{bmatrix} = \begin{bmatrix} \dot{\phi} \\ \frac{\cos \phi(-1.8u + 11.5v + 9.8 \sin \phi) - 10.9u + 68.4v - 1.2\dot{\phi}^2 \sin \phi}{\cos \phi - 24.7} \\ \frac{(9.3u - 58.8v) \cos \phi + 38.6u - 243.5v - \sin \phi(208.3 + \dot{\phi}^2 \cos \phi)}{\cos^2 \phi - 24.7} \end{bmatrix} \quad (41)$$

We use a 3 layer MLP as the controller. First, we train the controller to imitate a Linear Quadratic Regulator (LQR) controller. Then we jointly learn the Lyapunov function and finetune the weights in the MLP. Here we use standard linear layers rather than orthogonal layers, and control the empirical Lipschitz constant of the neural network by adversarial training.